Available online at www.pelagiaresearchlibrary.com

Pelagia Research Library

Advances in Applied Science Research, 2015, 6(3):72-82

ISSN: 0976-8610
CODEN (USA): AASRFC

Inter-band current and plasma on the surface of a semiconductor nanotube with longitudinal super-lattice

Ishaya Iliyasu

Department of Science Laboratory Technology, Nuhu Bamalli Polytechnic, School of Applied Sciences, Zaria, Kaduna, Nigeria

---

ABSTRACT

The collective oscillation of electrons in a nanotube was investigated theoretically. Kubo formula was analytically derived for electron gas conductivity tensor on the surface of a nanotube in a magnetic field. The plasma wave spectrum of an electron gas on a cylindrical surface with longitudinal superlattice was determined using the hydrodynamic approximation methods, considering time and spatial dispersion. Within the framework of this approach Poisson equation, continuity equation and constitutive equations were considered and the dispersion equation was obtained for the spectrum of plasma waves on the surface of a nanotube. The plasma waves, inter-band current and the spectra of waves on a semiconductor nanotube surface were considered. Because of the dispersion equation parameter in the spectrum of Plasma there exists, either one branch of the spectrum or two branches. The first branch describes optical Plasmon due to anti-phase oscillations of the electron density in the mini-bands involved in the transitions. The second branch of the acoustic is due to in phase oscillations of the electrons in the mini-bands. The study showed that the Plasma waves experiences Landau damping.

Keywords: Nanotubes, Plasmon, super-lattice, inter-band current, intra-band current, optical Plasmon, acoustic Plasmon.

INTRODUCTION

SumioIijima in 1991 discovered carbon nanotubes Ref. [13]. Together with fullerene and carbon mesoporous structures this formed a new class of nanomaterial whose properties differ significantly from those of other forms of carbon such as graphite and diamond. Currently, the physical properties are still being discovered and disputed. What makes it so difficult is that nanotube have a very broad range of electronic, thermal and structural properties that change depending on the different kinds of nanotube (defined by its diameter, length and chirality or twist). Currently there have been intensive studies of the properties of carbon nanotubes and semiconductor nanotubes. The energy spectrum of electrons on the surface of carbon nanotube is conical, and on the surface of the semiconductor nanotube (based on gallium arsenide and its derivatives) it's parabolic. There is increased interest in the semiconductor nanotubes due to the fact that they are widely used in Nano electronic devices. Modern state of the art physical experiment allows producing them in the laboratory.

Theoretical physicists are interested in improving the methods for the development of systems with planar geometry with two-dimensional electron gas on the surface of a cylinder. Presence in theory is a new parameter (the curvature structure) – this parameter increases the number of ways to control the properties of the system. A modern method of production of semiconductor nanotube allows you to create not only a nanotube, but a nanotube with super-lattice. There are radial Ref. [1, 4, 5, 6] and longitudinal, Ref. [7, 8] super-lattices with cylindrical symmetry. Radial superlattice is a set of coaxial cylinders, and is similar to the longitudinal stack of coaxial rings. The longitudinal superlattice is created by introducing fullerenes into the nanotube Ref. [7, 8].Usually it is included in the creation of fullerene nanotube, as a result, the energy spectrum of the longitudinal motion of electrons on the tube arises through narrow mini-bands, separated by energy gaps whose widths are defined by the modulating potential amplitude Ref. [9, 10]. The study of collective excitations in such systems has been a major task of Nano physicists.

In theory, the Plasmon on the tube usually uses hydrodynamic method Ref. [1] and the random phase approximation Ref. [2, 3]. But the hydrodynamic approach considers the Poisson equation for the plasma wave potential, the equation of continuity and the material equation relating the current density and electric field. Using these equations and the simplest expression for the conductivity, the authors of [1, 11] obtained the dispersion equation for the spectrum of surface plasma on the surface of the tube. The authors of [1] obtained a spectrum of intra-band and inter-band Plasmon on the tube without the superlattice. In the presence of the super-lattice, it's necessary to consider the inter-band current associated with the quantum electron transitions between mini-bands in the field of an electromagnetic wave. Considering this current, one can see that in the spectrum of Plasmon there exists either one branch of the spectrum, or two branches. In the latter case, one branch describes optical Plasmon due to anti-phase oscillations of the electron density in the mini-bands involved in the transitions. The second branch of the acoustic is due to in-phase oscillations of the electrons in the mini-bands. The corresponding branch of the spectrum lie outside the electron–hole continuum, therefore the plasma waves experiences Landau damping.

MATERIALS AND METHODS

- **The energy spectrum of electrons on the surface of the semiconductor nanotubes (quantum cylinder**).

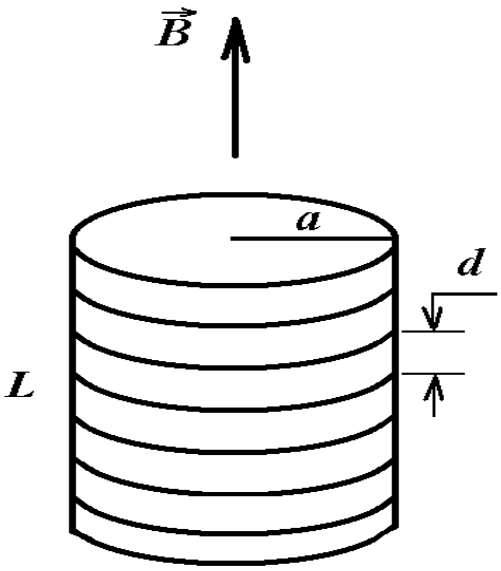

Fig.1. Electronic gas in the surface of a cylinder with radius a and length L

The band-structure effects take into account the introduction of the electron effective massm_*. The symmetry of the system allows you to find the conserved quantities: the projection of the angular momentum of the electron on the cylinder axis z, projection of the momentum $\hbar k(-\infty < k < +\infty)$ on this axis. The energy of the circular motion of the electron [12] $\frac{m^2}{2j}$ $(M = M_z = l\hbar, J = m_* a^2)$- moment of inertia of the electron) is equal to

$$\mathcal{E}_l = \frac{\hbar^2 l^2}{2m_* a^2} = \mathcal{E}_0 l^2$$

Where

$$\mathcal{E}_0 = \frac{\hbar^2}{2m_* a^2} \quad \text{-Rotational quantum.}$$

For gallium arsenide with $m_* \sim 10^{-28} g$ at $a \sim 10^{-7}$a rough estimate yields

$\varepsilon_0 \sim \frac{10^{-54}}{10^{-28}10^{-14}} erg \sim 10^{-12} erg.$

That corresponds to the temperature $\frac{10^{-6}}{10^{-14}} K = 100K.$

Energy of the longitudinal motion of the electron
$\varepsilon_k = \frac{\hbar^2 k^2}{2m_*}.$

Then the energy of an electron in a state |lk⟩ is
$\varepsilon_{lk} = \varepsilon_0 l^2 + \frac{\hbar^2 k^2}{2m_*}.$

Levels of circular motion are doubly degenerate (at $l \neq 0$) in the direction of the moment. Zero level ($l = 0$) is not degenerate.

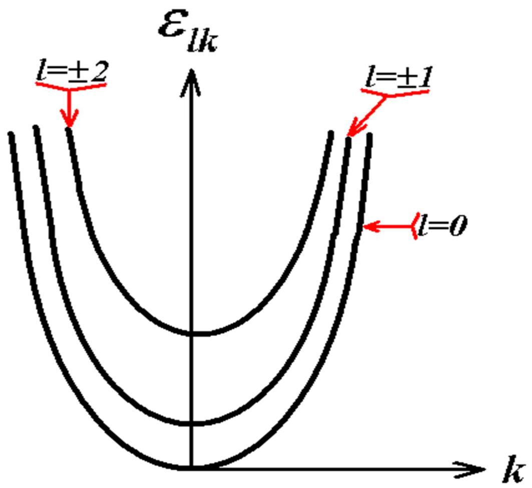

Fig.2. shows a parabola $\mathcal{E}_{lk}$ for several *l*.

The presence of the magnetic field along the axis of the induction tubes leads to an additional rotation of the electron tube in a clockwise direction or counter clockwise depending on the direction. As a result, the energy of the circular motion becomes equal to $\mathcal{E}_l = \mathcal{E}_0(l+\eta)^2$ [12], where $\eta = {}^{\Phi}/_{\Phi_0}$ and $\Phi = \pi a^2 B$-magnetic flux induction through the cross section of the tube, $\Phi_0 = {}^{2\pi c\hbar}/_{|e|}$-quantum flux. This follows from the Schrödinger equation in cylindrical coordinates.

$$\frac{1}{2m_*}\left(-i\hbar\nabla - \frac{e}{c}\vec{A}\right)^2\psi = \varepsilon\psi,$$

In the field ($\vec{B}$) the energy of electron is equal to $\varepsilon_{lk} = \varepsilon_0(l+\eta)^2 + \frac{\hbar^2 k^2}{2m_*}$ and the stationary state of the electron can be written as

$$\langle\varphi z|lk\rangle = \frac{e^{il\varphi}}{\sqrt{2\pi}}\frac{1}{\sqrt{L}}e^{ikz}.$$

Magnetic field shifts the ground level (l = 0) and splits the doubly degenerate levels (see Fig. 3). If $0 < \eta < \frac{1}{2}$, then $\mathcal{E}_l$ alternate as: $0 < \eta < \frac{1}{2}$,

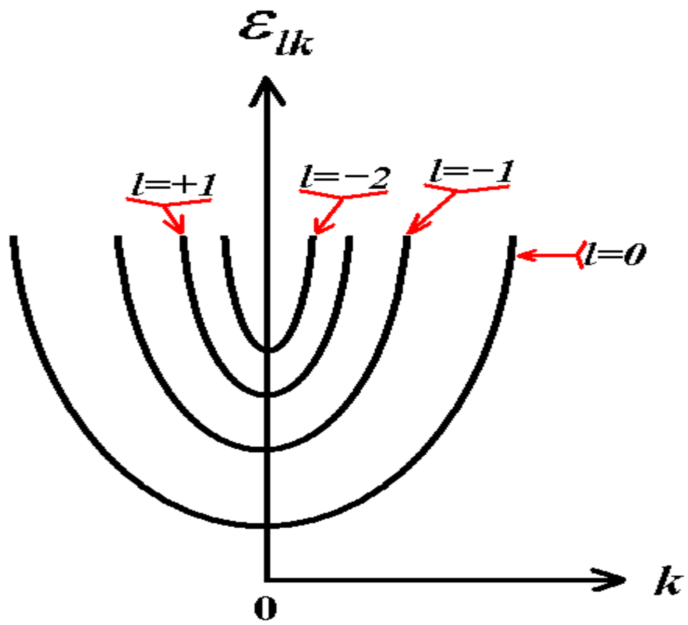

Fig 3.Energy levels spectrum

If $\frac{1}{2} < \eta < 1$, then the sequence of levels ε_l alternates also as: $\varepsilon_{-1} < \varepsilon_0\eta^2 < \varepsilon_{-2} < \varepsilon_1 <. . .$We estimate the field B, at which:

$\Phi = \Phi_0$: $B_m = \frac{2\pi c\hbar}{e\pi a^2} \sim \frac{10^{10}\times10^{-27}}{10^{-10}10^{-12}} Gauss \sim 10^5 Gauss.$

Reducing a 10 times increases B_m 100 times.$\eta \ll 1$in attainable fields.Fig. 3 shows the spectrum of electron energy at $\eta < 1/2$,

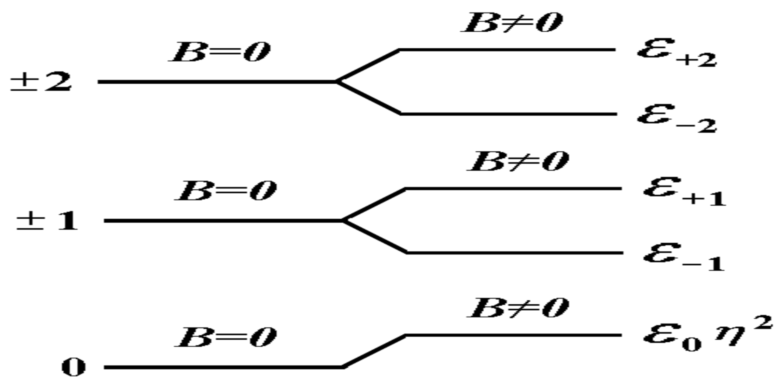

Fig.4. The energy level scheme in a longitudinal magnetic field

The Influence of longitudinal Super-lattice leads to the appearance of a periodic potential along the tube axis. Accounting for it in the strong coupling approximation gives the energy spectrum of electrons on the surface of the tube as:

$$\varepsilon_{lk} = \varepsilon_0(l+\eta)^2 + \Delta(1 - coskd), \quad (1)$$

Where Δ-amplitude of super-lattice and d - period of super-lattice (Fig.1.). If we execute $kd \ll 1$, we have

$\varepsilon_k = \frac{\hbar^2 k^2}{2m_*}$,

where $m_* = \frac{\hbar^2}{\Delta d^2}$.

We assume that the transverse (in $\mathcal{E}_k$) and longitudinal (in $\mathcal{E}_l$) effective masses are the same. Now the electron momentum $\hbar k$ becomes quasi-momentum and is limited to the first Brillouin zone: $-\pi / d \leq k \leq +\pi / d$. In the energy spectrum of electrons there appears mini-band of width 2Δ. The level scheme is shown in Fig. 5, at $\eta < 1/2$.

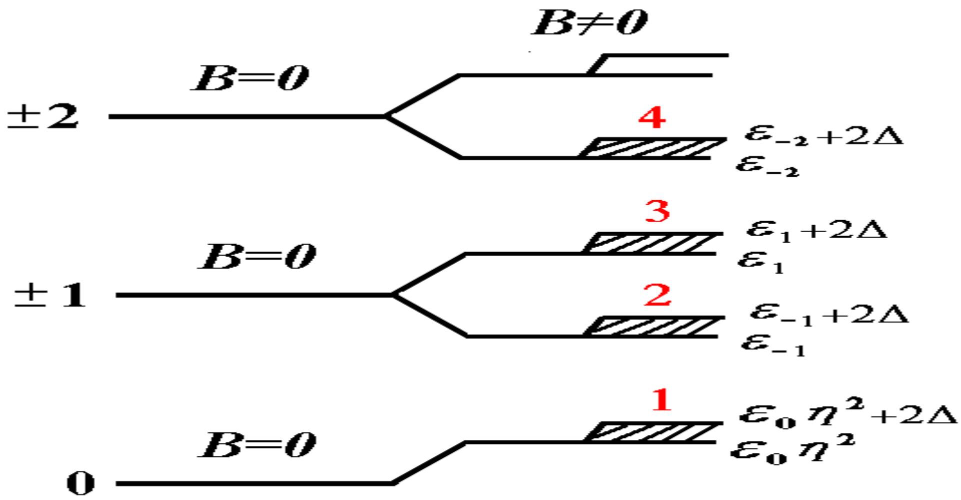

FIG.5.Energy spectrum of electrons with mini-band of width 2Δ

$\mathcal{E}_{lk}$dependence is shown in Fig. 6 in the first Brillouin zone $[-\pi / d, \pi / d]$. In case (a) there is no overlap of the mini-bands, and in case (b) they overlap.

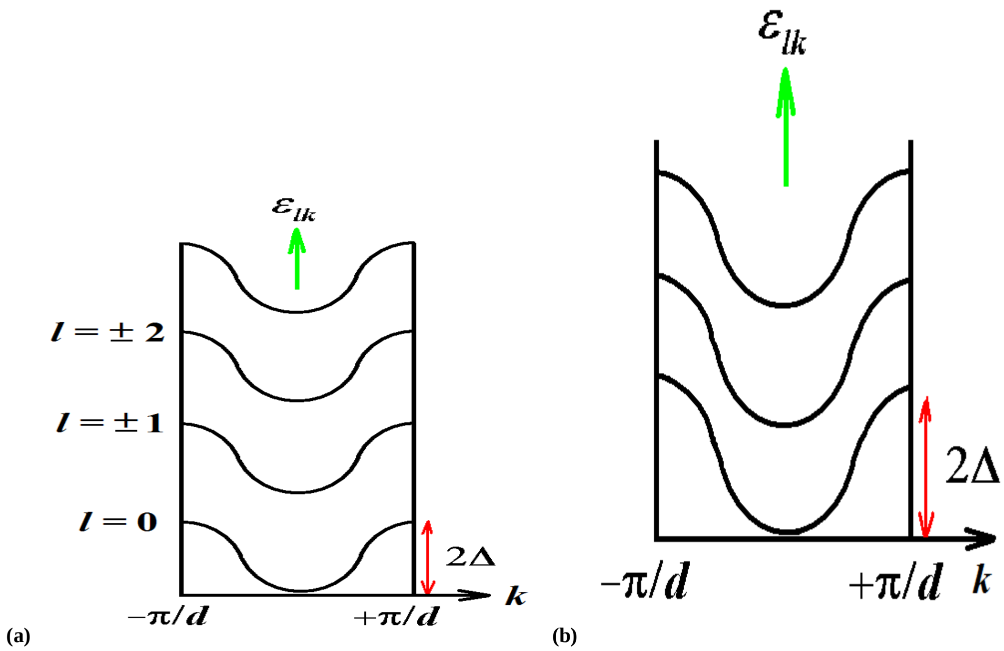

Fig 6. (a) No Overlap of the mini-bands (b) overlap of mini-band

Electron density of states has root singularities at the boundaries of the mini-band (see. Fig. 7 no-overlapping). The width of each of the mini-band is 2Δ.

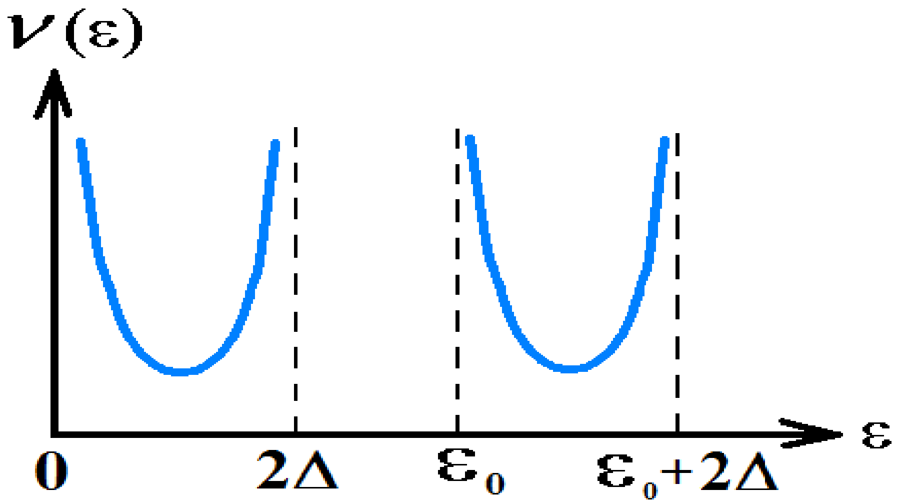

FIG 7 $v(\mathcal{E})$ vs $\mathcal{E}$ graph (no overlap)

RESULT AND DISCUSSION

This work is devoted to the study of the plasma spectrum on the surface of the semiconductor nanotube with a longitudinal super-lattice. The plasma on the tube is studied using hydrodynamic and random phase approximation methods. Hydrodynamic method was used for the first time in Ref. [1]. They used the Poisson equation for the scalar potential waveΦ

$$\Delta\Phi(\rho,\varphi,z,t) = -4\pi e\tilde{n}_s\delta(\rho - a) \tag{2}$$

whereρ, φ, z −cylindrical coordinate. Continuity equation has the form:

$$e\frac{\partial\tilde{n}_s}{\partial t} + div\,\vec{j}_s = 0 \tag{3}$$

Since

$$\vec{E} = -\nabla\Phi,$$

then the current density on the tube in the case of an isotropic quadratic dispersion law of electrons $\mathcal{E} = {}^{P^2}\!/_{2m_*}$ gives the material (constitutive) equation as

$$\vec{j}_s = -\sigma\nabla\Phi_{|\rho=a}$$

Where the Drude-Lorentz expression for conductivity σ was used, excluding the electron collisions:

$$\sigma = i\frac{e^2 n_s^0}{m_*\omega} \tag{4}$$

where n_s^0– equilibrium electron density. Taking into account the oscillations of the electron density we obtain $n_s = n_s^0 + \tilde{n}_s$. Here we use $e = -|\,e\,|$, n_s − surface electron density $\vec{j}_s$ – surface current density, $q$and ω – the wave number and frequency of the wave. Linearization of the system of equations (2), (3) for small oscillations

$(\tilde{n}_s << n_s^0)$

$$\sim e^{i(m\varphi + qz - \omega t)}. \tag{5}$$

The dispersion equation for density of oscillation of electron gas on a nanotube [1] with momentum projection q and angular momentum $m$in the absence of magnetic field (at$\vec{B} = 0$) has the form:

$$\omega = Im\sigma\left(\frac{m^2}{a^2} + q^2\right)4\pi a I_m(qa)K_m(qa) \tag{6}$$

Here $\hbar m$ and $\hbar q$ – angular momentum and momentum of Plasmon, I_m and K_m – modified Bessel functions.
The solution of equation (6) (at $\vec{B} = 0$) has the form:

$$\omega_m^2(q) = \frac{4\pi e^2 a n_s}{m_*}\left(\frac{m^2}{a^2} + q^2\right)I_m(qa)K_m(qa) \tag{7}$$

At $m = 0$ the solution for the dispersion equation for the electron density oscillation in axial symmetry represent the spectrum of intra-band Plasmon i.e. the wave amplitude propagated along the tube does not depend on the polar angle. There exist also the solution of the dispersion equation at $m = \pm1, \pm2, \ldots$ corresponds to interband plasma. However at $m \neq 0$, there exists a quantum transition of electrons in the wave field between minibands. Substituting the Drude-lorentz expression for conductivity (4) into equation (6), we obtain the known spectrum for inter-band and intra-band Plasmon

$$\Omega_{mq}^2 = \frac{4\pi e^2 a n}{m_*}\left(\frac{m^2}{a^2} + q^2\right)I_m(qa)K_m(qa). \tag{8}$$

We used Kubo method to calculate the inter-band current and obtained the transverse conductivity

$$Im\sigma_\perp(m,\omega) = \frac{e^{2n_s}}{m_*\omega} + \frac{e^2\hbar k_0 m^2\omega_m}{2\pi^2 m_*^2 a^3\omega(\omega^2 - \omega_m^2)} \tag{9}$$

and longitudinal conductivity

$$Im\sigma_\parallel = \frac{e^2 n_s}{m_*\omega} + \frac{2e^2\hbar k_0{}^3\omega_m}{3\pi^2 m_*{}^2 a\omega(\omega^2 - \omega_m^2)}, \tag{10}$$

where$\omega_m = {}^1\!/_{\hbar}\, \varepsilon_0 m^2$– the frequency of direct transitions of electrons between mini-bands $0 \longrightarrow m$, $m = \pm1, \pm2, \ldots$..

In formulas (9) and (10) at temperature $T = 0$ only the lower mini-band with number $l = 0$ is filled. We have not taken into account the spatial dispersion ($qv_F \ll \omega$) conductivity. In Fig. 8 the transitions with $m \neq 0$ is shown, when there is no overlap of mini-band. Here $\mu -$ the Fermi energy,

$\hbar k_0 = {}^{\hbar}\!/_{d}\, arccos\, {}^{\Delta - \mu}\!/_{\Delta}$ –the maximum momentum of the electrons in the mini-band when $l = 0, n_s < 1/\pi ad$. There exists a connection n_s with k_0:

$$n_s = \frac{k_0}{\pi^2 a}, \; l = 0.$$

We have included formula (9) and (10) into the dispersion equation (6) and obtained the following result. It turned out that the solution depends on the dispersion equation parameter:

$$\alpha_m = \frac{3m^2}{4\pi^4 a^4 n_s{}^2},$$

This characterizes the oscillator strength for resonance transitions $0 \rightarrow m$ of electrons between the mini-bands.

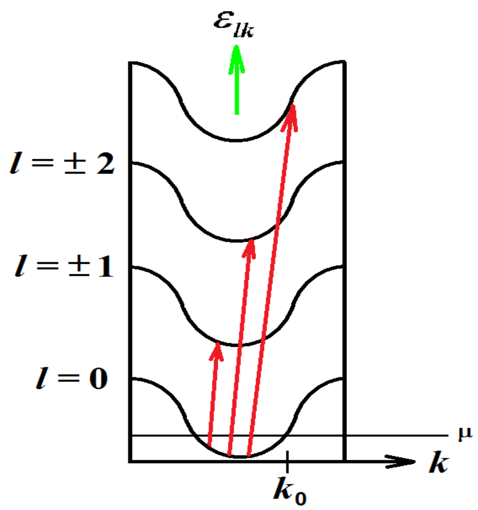

Fig.8. Inter-band energy spectrum transition when $m \neq 0$

Normal, Optical and Acoustic dispersion spectrum

If $\alpha_m < 1$, there is one root dispersion equation above ω_m

$$\omega^2{}_m(q) = \frac{1}{2}\left[\omega^2{}_0 + \omega^2{}_m + \sqrt{(\omega^2{}_0 + \omega^2{}_m)^2 + \frac{4}{\alpha}\omega^2{}_0\omega^2{}_m \frac{q^2a^2}{m^2}\frac{1-\alpha}{1+{q^2a^2}/{m^2}}}\right]. \quad (11)$$

Here ω_0^2 equals equation (8), $\omega_m = \frac{1}{\hbar}\varepsilon_0 m^2$ - The frequency of the single-particle electron transitions electron $0 \rightarrow m$. Fig. 9 shows the frequency of the wave (11) $\omega'_{1q} = {\omega_{1q}}/{\Omega_{10}}$ (solid line) and wave (8) $\Omega'_{1q} = {\Omega_{1q}}/{\Omega_{10}}$ (dashed curve) as a function of $x = qa$ for $m = 1$and $\alpha_1 = 0.75$. Here $\Omega_{10} = \left({2\pi e^2 n}/{m_* a}\right)^{1/2}$ – limiting frequency for the wave with the spectrum (8). Parameter values $m_* = 0.64 \cdot 10^{-28} g$ (GaAs), $a = 10^{-7}$ cm, $k_0 a = 1$ are used. Under the condition $\alpha_1 < 1$ the Fermi level lies in the upper half of the mini-band.

If $\alpha_m > 1$ we get two branches connected with each $0 \rightarrow m$ transition:

$$\omega^2{}_\pm(m,q) = \frac{1}{2}\left[\omega^2{}_0 + \omega^2{}_m \pm \sqrt{(\omega^2{}_0 + \omega^2{}_m)^2 - \frac{4}{\alpha}\omega^2{}_0\omega^2{}_m \frac{q^2a^2}{m^2}\frac{\alpha-1}{1+{q^2a^2}/{m^2}}}\right]. \quad (12)$$

Fig. 10 shows the dependence of the wave frequencies (12) $\omega'_\pm(1,q) = {\omega_\pm(1,q)}/{\Omega_{10}}$ (solid and dashed-dotted curves) and wave (8) $\Omega'_{1q} = {\Omega_{1q}}/{\Omega_{10}}$ (dashed curve) as a function of $x = qa$ under $m = 1$and $\alpha_1 = 3$. The above mentioned values of m_*, a and $k_0 a = 0.5$ were used. In this case the Fermi level lies in the lower half of the mini-band.The branches (11) and ω_+ (12) are positioned above ω_m, and the branches ω_- (12) are below ω_m.

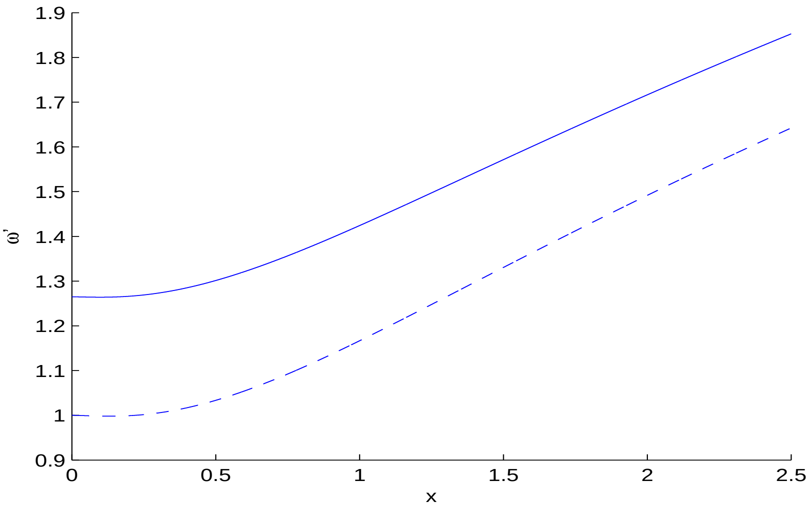

Fig.9 the dispersion curves of waves with spectrum (11) (solid line) and with spectrum (8) (dashed line) under $m = 1, \alpha_1 < 1$

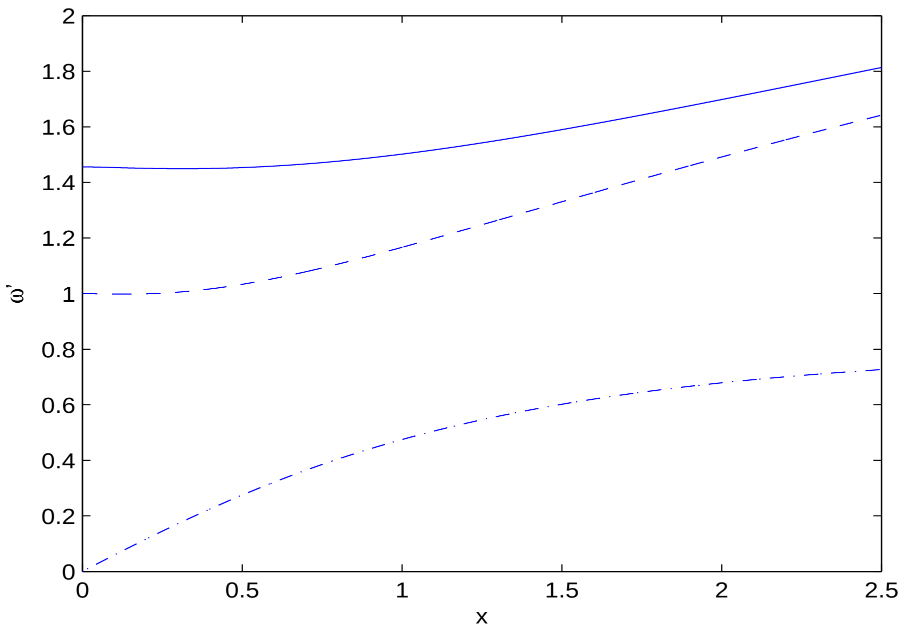

Fig.10. the dispersion curves of waves with the spectrum (12) (solid and dashed-dotted curves) and with spectrum of (8) (dashed lines) under $m = 1, \alpha_1 > 1$

In the limit of long waves($qa \ll 1$, and at $\alpha_m < 1$)from Equation (11), we obtain

$$\omega_{1q}^2 = \omega_{10}^2 \left[1 + \frac{1}{2} \frac{\Omega_{10}^2}{\omega_1^2 + \Omega_{10}^2} (qa)^2 \ln qa + \frac{4}{3} \frac{\omega_1^2 \Omega_{10}^2}{\left(\omega_1^2 + \Omega_{10}^2 \right)^2} (1 - \alpha_1)(k_0 a)^2 (qa)^2 \right], \tag{13}$$

$$\omega^2{}_{mq} = \omega^2{}_{m0} [1 + \frac{\Omega^2{}_{m0}}{\omega^2{}_m + \Omega^2{}_{m0}} \frac{m^2 - 2}{2m^{2(m^2-1)}} (qa)^2 + \frac{4}{3m^4} \frac{\omega^2{}_m \Omega^2{}_{m0}}{(\omega^2{}_m + \Omega^2{}_{m0})(1 - \alpha_m)(k_0 a)^2 (qa)^2}]. \tag{14}$$

the critical frequencies of waves with spectra (13) and (14) are

$$\omega_{m0}^2 = \omega_m^2 + \Omega_{m0}^2 = \varepsilon_0^2 m^4 + \frac{2e^2 k_0 |m|}{\pi m_* a^2}, \tag{15}$$

where $\sqrt{2 \frac{\pi e^2 n_s}{m_* a} |m|}$ - frequency depolarization shift. As n_s depends on k_o then this shift can be judged on the parameters of the superlattice Δ (period) and d (modulating frequency).

At $\alpha_m > 1$, the expressions (13) and (14) are true for the upper branch ω_+. The bottom branch ω_- has the sound spectrum $\omega_- (m, q) = c_m q$, where

$$c_m^2 = \frac{4a^2}{3m^4} (k_0 a)^2 \frac{\omega_m^2 \Omega_{m0}^2}{\omega_{m0}^2} (\alpha_m - 1). \tag{16}$$

Optical ω_+ and acoustic ω_- branches are connected with in-phase and anti-phase density oscillations of electrons which participate in longitudinal and transversal motion on the tube.

CONCLUSION

This work is devoted to the study of Plasmon spectrum on the surface of semiconductor nanotube with a longitudinal superlattice. Plasmon on the tube was studied by the hydrodynamic approximation method. In studying the propagation of electromagnetic waves on the surface of a semiconductor nanotube the understanding of the electron gas conductivity tensor components is worthwhile, noting that the field nature in the tube and characteristics wave properties are responsive to the surface current. This work showed that with an understanding of the conductivity tensor the data of an electron gas can be obtained. The study showed that the Plasmon waves experiences Landau damping.

The main results of this work are following:
1. Obtained Kubo formula for the conductivity tensor of the electron gas on the surface of the nanotube.
2. Obtained dispersion equation for the spectra of plasma waves on the surface of nanotubes using hydrodynamic approach.
3. Calculated spectra of Plasmon on the surface of the semiconductor nanotubes with longitudinal superlattice.
4. Show that both optical and acoustical Plasmon could propagate along the tube with one sort of carriers.
5. Optical ω_+ and acoustic ω_- branches are connected with in-phase and anti-phase density oscillations of electrons which participate in longitudinal and transversal motion on the tube.

Acknowledgement
I am grateful to Dr G.I Rashba and Professor A.M. Ermolaev for the entire support in this work and the department of Theoretical Physics (academician I.M. Lifshits) V.N. Karazin Kharkov National University Ukraine.

REFERENCES

[1] Vedernikov A.I, Govorov A.O, Chaplik A.V, JEPT **2001**,120, 979.
[2] Vitlina R.Z, Magarill L.I,Chaplik A.Z,*JETP***2008**, *vol* 133, 906-913.
[3] Ermolaev A.M, Rashba G.I, Solyanik M.A. *Physica***2011**, *vol* B406, 2077-2080.
[4] Lin M.F, Shung K.W. *Phys. Rev.***1993**, *vol* B47, 6617-6624.
[5] Longe P, Bose S.M, *Phys. Rev.***1993**, *vol* B48, 18239-18243.
[6] C Yannoules C, E.N Bogachek E.N, Landman U. Phys. Rev. B53 **1996**, 10225–10236.
[7] Lee J, Kim. H, Khang S.J, KimG, Son Y.W, Kato H, Wang Z.W, Okazi T, Shinohara H, Kuk Y, Nature 415 **2002** 1005-1008.
[8] Shin H.J, Clair S, Kim Y, Kawai M, *Nature nanotech*, 4 **2009** 567-570.
[9] Ermolaev A.M, Rashba G.I, M.A.Solyanik M.A, . *Low Temp. Phys*,**2012**, *vol* 38, 957-964.
[10] Ermolaev A.M, Rashba G.I, SolyanikM.a,.*Low Temp. Phy*, **2012**, *vol* 38, 511-516.
[11] Eminov P.A, Perepelkina Y.V. *Phys. Solid State*,**2008**, *vol* 50, 2220-2224.
[12] Magarill L.I, Chaplik A.V, Entin M.V. *Spectrum and kinetics of electrons in curved nanostructures*, UspekhiFizicheskikhNauk,**2005**, *vol* 175, 995-1000.
[13] Iijima S, *Helical microtubules of graphitic carbon*,Nature,**1991**, vol. 354, pp. 56-58.